Inorganic Chemistry

Article

pubs.acs.org/IC

Water-Stable Manganese(IV) Complex of a N_2O_4-Donor Non-Schiff-Base Ligand: Synthesis, Structure, and Multifrequency High-Field Electron Paramagnetic Resonance Studies

Malay Dolai,[†,‡] Asma Amjad,[‡,§] Mainak Debnath,[†] Johan van Tol,[⊥,∥] Enrique del Barco,*[,§] and Mahammad Ali*[,†]

[†]Department of Chemistry, Jadavpur University, Kolkata 700 032, India

[§]Department of Physics, University of Central Florida, Orlando, Florida 32816, United States

[⊥]National High Magnetic Field Laboratory (NHMFL), Florida State University, Tallahassee, Florida 32310, United States

[∥]Department of Physics, Florida State University, Tallahassee, Florida 32310, United States

Supporting Information

ABSTRACT: A novel water-stable ($t_{1/2}$ ~ 6.8 days) mononuclear manganese(IV) complex of a hexacoordinating non-Schiff-base ligand (H_4L) with N_2O_4-donor atoms has been synthesized and characterized crystallographically. High-frequency electron paramagnetic resonance experiments performed on a single crystal reveal a manganese(IV) ion with an $S = {}^3/_2$ ground spin state that displays a large single-ion anisotropy, setting the record of mononuclear manganese(IV) complexes reported so far. In addition, spin−echo experiments reveal a spin−spin relaxation time T_2 ~ 500 ns.

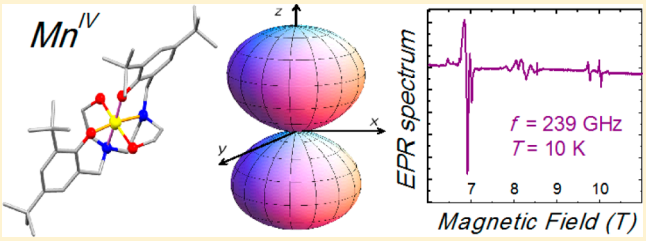

INTRODUCTION

Manganese is an essential component of various biological redox processes, viz., in catalases[1] and in oxygen-evolving photosystem II (PS-II),[2,3] where the active intermediate generated is believed to have manganese in the +4 oxidation state. Hence, the studies associated with manganese(IV) are important in bioinorganic chemistry. Manganese(IV) is also relevant in molecular magnetism because it is a constituent of some crucial single-molecule magnets (SMMs).[4] Although a number of oxo-bridged multinuclear manganese(IV) complexes are known to be stable enough for the successful study of their solution chemistry, mononuclear nonoxomanganese(IV) complexes that are stable in an aqueous medium have been scarcely reported.[5] This situation has considerably limited our knowledge of the aqueous chemistry of Mn^{IV}, a key species in PS-II. The first structurally characterized mononuclear manganese(IV) complexes were reported independently by the Pierpont,[6] Christou,[7] and Pecoraro[8,9] groups in the 1980s. These compounds have been critical to the understanding of Mn^{IV} in biology because they provide detailed electron paramagnetic resonance (EPR) spectral evaluation of Manganese(IV). A CSD search (CSD version 5.35, Nov 2013) on MnN_2O_4 coordination resulted in 1917 hits, out of which only 34 were found to be based on mononuclear manganese(IV) complexes. Again, out of these 34 hits only 8 complexes were found to be of non-Schiff-base ligands,[10] but none of these were found to be water-stable. Only one complex of the biguanide ligand in the N_2-donor environment, $[Mn^{IV}(bigH)_3]^{4+}$, was found to be water-stable.[5]

However, there were only a few manganese(IV) Schiff base complexes that were either isolated from or reacted in aqueous media.[11]

The magnetostructural properties of mononuclear manganese(IV) complexes ($S = {}^3/_2$), such as zero-field splitting (zfs), are of great interest. However, despite numerous X-band (9.4 GHz) EPR studies of such complexes, a precise determination of these parameters has been scarce.[12−15] The zfs values of Manganese(IV) impurities in magnesium and aluminum oxide are exceptions, while the record zfs value found for Manganese(IV) remains D = 1.6 cm^{-1}.[15] In this paper, we disclose an aqueous stable manganese(IV) complex, which happens to have a record magnetic anisotropy, as delineated by single-crystal high-frequency EPR studies.

EXPERIMENTAL METHODS

Chemicals and Reagents. The starting materials for synthesis of the H_4L ligand, viz., 2,4-di-*tert*-butylphenol (Lancaster), formaldehyde (Merck India), and *N*,*N*-bis(2-hydroxyethyl)ethylenediamine (Aldrich Chemicals), were of reagent-grade and were used as received. $MnCl_2 \cdot 4H_2O$, triethylamine (TEA), and solvents like ethanol, petroleum ether, and methanol (MeOH; Merck India) were of reagent-grade and were dried by standard methods before use.

Received: September 13, 2013
Published: May 13, 2014

   dx.doi.org/10.1021/ic4030958 | Inorg. Chem. 2014, 53, 5423−5428

Synthesis of the H_4L Ligand. The ligand (H_4L) was prepared by using simple Mannich condensation.[16] In a typical procedure, *N,N*-bis(2-hydroxyethyl)ethylenediamine (2.22 g, 15 mmol) in 50 mL of MeOH along with 2,4-di-*tert*-butylphenol (6.19 g, 30 mmol) and formaldehyde (3 mL, 41%, 35 mmol) was stirred for 2 days. The solution was kept in air to partially evaporate the solvent (about 20 mL). A white solid appeared within 2 days. After filtration, the solid was washed with cold MeOH and dried in air.

Synthesis of Complex [Mn(L)]. $MnCl_2$ (0.039 g, 0.20 mmol) was dissolved in 20 mL of MeOH, and then hexadentate H_4L (0.117 g, 0.20 mmol), deprotonated separately by treatment with TEA (0.081 g, 0.80 mmol) in MeOH, was added to this solution with stirring. The dark-pink color of the solution appeared almost immediately. Stirring was continued for 1 h and then filtered off. The filtrate was kept aside undisturbed for slow evaporation. After the mother liquor was allowed to stand for 2 days, dark-pink rod-shaped crystals were obtained and collected by filtration. The isolated suitable single crystals were subjected to X-ray studies. Elem anal. Calcd: C, 68.00; H, 8.87; N, 4.40. Found: C, 67.8. H, 8.79; N, 4.50.

Crystallography. Single-crystal X-ray data of the complex was collected on a Bruker SMART APEX-II CCD diffractometer using graphite-monochromated Mo Kα radiation (λ = 0.71073 Å). Data collection, reduction, structure solution, and refinement were performed using the Bruker *APEX-II* (v2.0-2) program suite. All available reflections to $2\theta_{max}$ were harvested and corrected for Lorentz and polarization factors with Bruker *SAINT plus*. Reflections were then corrected for absorption, interframe scaling, and other systematic errors with *SADABS*. The structures were solved by direct methods and refined by means of a full matrix least-squares technique based on F^2 with the *SHELX-97* software package.[17] All of the non-hydrogen atoms were refined with anisotropic thermal parameters. All of the hydrogen atoms belonging to carbon atoms were placed in their geometrically idealized positions. Drawings of the molecules were generated with the *PLATON-1.16* and *Mercury 2.4* programs. The crystallographic data are given in Table 1.

Table 1. Crystal Data and Structure Refinement of the Complex 1

empirical formula	C_{36} H_{56} Mn N_2 O_4(ccdc no.-947606)
fw	635.77
temperature (K)	273
wavelength (Å)	0.71073
cryst syst	monoclinic
space group	*P*21/*c* (No. 14)
unit cell dimensions	
a (Å)	14.0488(4)
b (Å)	9.9929(3)
c (Å)	24.7991(7)
α (deg)	90.00
β (deg)	93.193(2)
volume (Å^3)	3476.10(17)
Z	4
density (calcd) (g cm^{-3})	1.215
abs coeff μ(Mo Kα) (mm^{-1})	0.419
F(000)	1372
cryst size (mm^3)	0.10 × 0.14 × 0.18
index ranges	−18:18, −13:13, −32:32
θ range for data collection	1.6−27.6°
total, unique data, *R*(int)	55622, 8062, 0.085
obsd data [$I > 2.0\ \sigma(I)$]	5626
completeness (%) to θ = 27.6°	100
abs corrn	empirical
no. of ref, no. of param	8062, 400
GOF on F^2	1.04
final *R* indices [$I > 2\sigma(I)$]	R1 = 0.0493, wR2 = 0.1306

EPR Spectroscopy Measurements. The magnetic properties of the complex were probed via multifrequency single-crystal high-field EPR (HF-EPR) studies. The experiments were conducted at the Electron Magnetic Resonance (EMR) Facility at the NHMFL (Tallahassee, FL). A heterodyne quasi-optical spectrometer equipped with a 12.5 T superconducting magnet was used for single-crystal measurements at high frequencies (>230 GHz).[18,19]

RESULTS AND DISCUSSION

The complex was prepared by the reaction of $MnCl_2$ in 20 mL of MeOH with H_4L (obtained from our previous work; Scheme 1)[16] in 20 mL of MeOH in the presence of TEA. The colorless solution immediately transformed to dark purple, yielding dark-purple rod-shaped crystals suitable for single-crystal X-ray studies after 2 days. Single-crystal X-ray diffraction analysis reveals that the compound crystallizes in a monoclinic *P*21/*c* space group. The compound is a monomeric neutral species, [Mn^{IV}(L)], in which the manganese(IV) ion has a highly distorted octahedral geometry with four oxygen and two nitrogen atoms of the L^{4-} ligands coordinated to a manganese atom, which creates a C_2 symmetry axis along the N−Mn−N axis (selected Mn−N1 and Mn−N2 bond lengths and angles are given in Table 2). The six coordination positions are occupied by atoms O1 and O4 (alkoxo oxygens), O2 and O3 (phenoxo oxygens), and N1 and N2 (amine nitrogens) of the ligand L^{4-}. The phenolic oxygen atoms are trans to the nitrogen atoms, while alkoxides are cis. The axial oxygen atoms (O1 and O4) have distances of 1.890 and 1.864 Å from the manganese(IV) center, while in the basal plane, the Mn^{IV}−O*i* (*i* = 2 and 3) distances are 1.849 and 1.865 Å and Mn^{IV}−N*i* (*i* = 1 and 2) are 2.076 and 2.060 Å, respectively. The four opposite bond angles around the manganese center at the basal plane, namely, O3−Mn−N2 (89.91°) versus N1−Mn−O2 (91.32°)

Scheme 1. Hexadentate H_4L Ligand

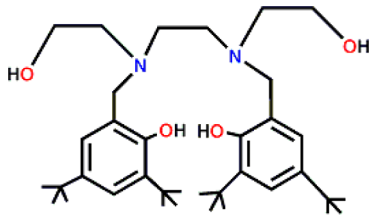

Table 2. Important Bond Lengths (Å) and Angles (deg) of Compound 1

Bond Distances			
Mn1−O1	1.8898(16)	Mn1−O3	1.8647(15)
Mn1−O2	1.8492(16)	Mn1−N1	2.0763(18)
Mn1−O4	1.8641(17)	Mn1−N2	2.0600(18)
Bond Angles			
O1−Mn1−O2	95.80(7)	O1−Mn1−N1	81.82(7)
O1−Mn1−O3	91.70(7)	O1−Mn1−N2	90.35(7)
O1−Mn1−O4	168.87(7)	O2−Mn1−N1	91.32(7)
O2−Mn1−O4	91.28(7)	O2−Mn1−N2	172.94(7)
O2−Mn1−O3	93.36(7)	O3−Mn1−N1	172.37(7)
O3−Mn1−O4	96.45(7)	O4−Mn1−N1	89.46(7)
O3−Mn1−N2	89.91(7)	N1−Mn1−N2	86.11(7)
O4−Mn1−N2	82.13(7)		

dx.doi.org/10.1021/ic4030958 | *Inorg. Chem.* 2014, 53, 5423−5428

and O3−Mn−O2 (93.36°) versus N1−Mn−N2 (86.1°), are nearly identical.

The molecular view of the complex in the crystallographic *ac* plane (see Figure 1) shows two different orientations (A and B)

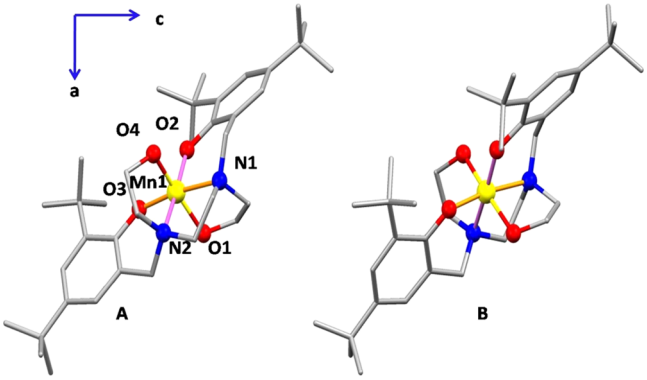

Figure 1. Molecular views of the manganese(IV) complex in the crystallographic *ac* plane showing the two different molecular orientations (A and B), related by mirror reflection about the *ac* plane. Hydrogen atoms are omitted for clarity. Symmetry operators: a, *x*, *y*, *z*; b, −*x*, 0.5 + *y*, 0.5 − *z*; c, −*x*, −*y*, −*z*; d, *x*, 0.5 − *y*, 0.5 + *z*.

of the molecules within the crystal, related to each other by reflection symmetry about the mirror plane *ac*. Strong hydrogen-bonding interactions are presented in Figure S1 in the SI, which leads to a 1D chain (Figure S2 in the SI). The bond valence sum (BVS) of the manganese ion was calculated to be 3.97, which is consistent with the +4 oxidation state of the central manganese atom (Table S2 in the SI). The stability of the complex was determined spectrophotometrically and found to be $k_d = 1.17 \times 10^{-6}$ s^{-1} in 50% (v/v) MeOH−H_2O (Figure S3 in the SI), which indicates fair stability of the complex in an organic aqueous medium with $t_{1/2} \sim 6.8$ days.

Single-Crystal EPR Spectroscopy. HF-EPR experiments have been performed in a single crystal of the mentioned compound. The study reveals spectra containing sharp resonances that can be directly associated with the spin $^3/_2$ system, hence allowing precise comparisons with theoretical simulations. A detailed study of the angular dependence of the EPR spectra for this sample has been conducted at two frequencies, 239 and 336 GHz. As will be shown below, the angle-dependent EPR study of the ground-state transition within the $S = {}^3/_2$ multiplet reveals an axial magnetic symmetry with an easy-anisotropy plane perpendicular to the *z* axis (hard axis). Figure 2a shows a sketch representing the magneto-anisotropic energy of the molecular spin. The 239 GHz EPR spectrum obtained at 10 K with the field along the easy-anisotropy plane (perpendicular to the *z* axis) is shown in Figure 2b. Three strong absorption peaks are observed at ∼6.9, ∼8.5, and ∼10 T, with the lowest-field peak displaying the highest intensity, as expected from a positive axial anisotropy parameter ($D > 0$) for this orientation of the magnetic field. The multiplicity of the peaks results from the two molecular orientations within the sample, as discussed below. No more peaks appear at fields below the range given in the figure.

The EPR spectra obtained in our study can be simulated by a complete diagonalization of the spin Hamiltonian:

$$H = DS_{z^2} + g\mu_B \mathbf{B}\cdot\mathbf{S} \qquad (1)$$

where *D* is the axial zfs parameter. The corresponding values of the parameters used to fit all of the data in this article are $S = {}^3/_2$, $D = 1.65$ cm^{-1}, and isotropic $g = 2$. For the data presented in this work, which is taken at high frequencies (i.e., EPR transitions occur at fields far from anticrossings between opposite spin levels; see Figure 2c), the effect of a reasonable rhombic anisotropy term, $E(S_{x^2} - S_{y^2})$, would be completely negligible; thus, it is not included in eq 1. Note that the value of the zfs parameter ($D = 1.65$ cm^{-1}) is larger than those previously reported in the literature.[12−15] Figure 2 shows the Zeeman energy levels of the Mn^{IV} ion as a function of the field applied along both the hard-anisotropy axis (*z* axis) and the easy-anisotropy plane (perpendicular to the *z* axis) calculated by direct diagonalization of the Hamiltonian in eq 1 using the parameters given above. The arrows indicate the three main expected transitions for 239 GHz, which are observed in the experiment (see Figure 2b for the $H \perp z$ case), corresponding to transitions between consecutive m_s levels within the $S = {}^3/_2$ multiplet. In particular, the three transitions observed with the field applied within the easy-anisotropy plane correspond to $m_s = (-{}^3/_2 \rightarrow -{}^1/_2)_\perp$ (∼6.9 T), $m_s = (-{}^1/_2 \rightarrow {}^1/_2)_\perp$ (∼8.5 T), and $m_s = ({}^1/_2 \rightarrow {}^3/_2)_\perp$ (∼10 T). The fact that the strongest EPR absorption peak corresponds to the lowest-field transition indicates that the axial anisotropy parameter *D* is positive, resulting in a hard-anisotropy axis along the *x* axis (i.e., an easy-anisotropy *xy* plane). Note that when the field is applied along the *z* axis, $m_s = (-{}^3/_2 \rightarrow -{}^1/_2)_\parallel$ becomes the highest-field transition, as seen in Figure 2c, while $m_s = ({}^1/_2 \rightarrow {}^3/_2)_\parallel$ becomes the lowest-field one. As shown below, the angular modulation of the main EPR transitions can be employed to determine the anisotropy parameters of the molecules with a high degree of accuracy.

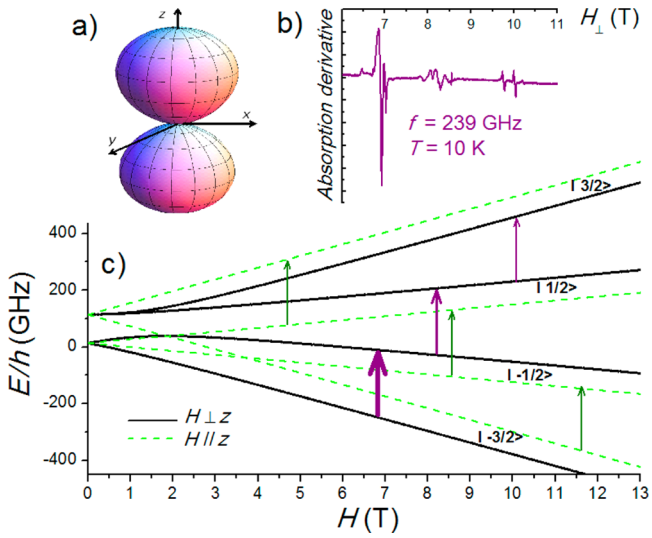

Figure 2. (a) Representation of the axial magnetoanisotropy energy of the molecular spin, which shows an easy magnetic *xy* plane. (b) Single-crystal spectrum observed at 239 GHz and 10 K, with the external magnetic field applied within the easy-anisotropy plane. (c) Zeeman energy diagram of the spin levels of Mn^{IV} with the field applied along both the hard-anisotropy *z* axis (dashed green lines) and the easy-anisotropy *xy* plane (continuous black lines) of the molecule. The expected transitions induced by microwaves of frequency 239 GHz are indicated by arrows (purple arrows indicate the absorptions shown in panel b).

In order to establish the direction of the anisotropy axes within the crystal, EPR spectra have been recorded at different orientations of the magnetic field with respect to the crystal faces. Figure 3 shows the angular dependence of the ground-

dx.doi.org/10.1021/ic4030958 | Inorg. Chem. 2014, 53, 5423−5428

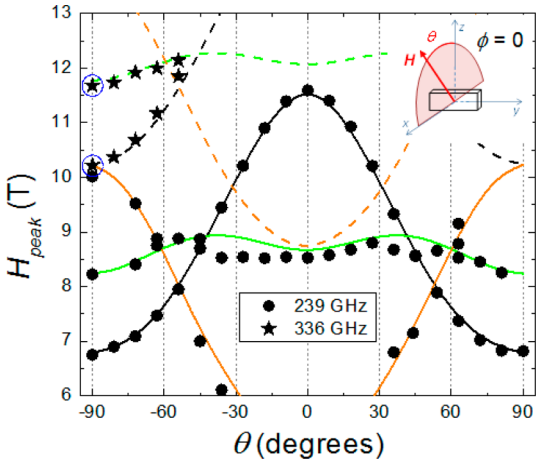

Figure 3. Angle dependence of the main EPR peaks observed at 10 K for a frequency of 239.2 (circles) and 336 GHz (stars). The field is rotated in a plane perpendicular to the long crystal axis (see the sketch). The lines represent the calculated response obtained from diagonalization of the Hamiltonian in eq 1

state EPR transition at 239.2 GHz (circles) and 336 GHz (stars), with the magnetic field rotated in a plane that is related to the crystal faces, as depicted in the sketch of Figure 3. The crystal is oriented such that the *y* axis lies along the longest crystal axis and the *x* axis is perpendicular to the flattest crystal face. This measurement corresponds to the external magnetic field being rotated at an angle θ from the *z* axis within the *zx* plane (ϕ = 0; red plane in Figure 3). The three main direct transitions within the $S = {}^3/_2$ multiplet can be followed in the response recorded at the lowest frequency (239 GHz). Only two transitions were observed within the field range of the experiment (<12 T) for the highest frequency (336 GHz). The lines in Figure 3 represent the calculated behavior of the respective transitions obtained by diagonalization of the Hamiltonian in eq 1 with the parameters given above (see below for more details). Specifically, $m_s = (-{}^3/_2 \rightarrow -{}^1/_2)$ is indicated with black lines, $m_s = (-{}^1/_2 \rightarrow {}^1/_2)_\perp$ with green lines, and $m_s = ({}^1/_2 \rightarrow {}^3/_2)$ with orange lines, using continuous and dashed lines for 239 and 336 GHz, respectively.

As mentioned before, one could clearly observe a 2-fold modulation of the main $m_s = (-{}^3/_2 \rightarrow -{}^1/_2)$ spin transition, with minima at $\theta = \pm 90°$ and a maximum in the peak field position when the field is applied along the *z* axis (θ = 0°), which corresponds to the hard-anisotropy axis (see below for details). The strong anisotropic nature of this molecule is evident from the strong modulation of the main EPR absorption, which shifts by almost 5 T between the easy-anisotropy plane (6.8 T for 239 GHz) and the hard-anisotropy axis (11.5 T for 239 GHz), giving this compound the record zfs value within other mononuclear manganese(IV) systems. The octahedral coordination of this molecule is strongly distorted by the disposition of the two large Mn−N bonds, significantly lowering the molecular symmetry. In fact, it is likely that the axial anisotropy axis of the molecule originates from the deformation produced by these bonds and may lie within the plane formed by N1−Mn−N2. This plane is tilted away from the crystallographic *ac* plane by 15.85° for one of the molecular orientations, while for the other orientation, the N1−Mn−N2 plane results from reflection on the opposite site of the *ac* mirror plane; i.e., the two distinct N1−Mn−N2 planes are titled by 31.70° with respect to each other (see Figure 1). If this is so and each molecular orientation has the anisotropy axis at a different direction, their EPR responses should be different for a given orientation of the applied magnetic field, unless the field is applied along the *ac* plane, which is the molecular mirror plane. Because all of the EPR peaks in Figure 3 follow approximately the same angular dependence, we conclude that the *zx* rotation plane coincides with the crystallographic *ac* plane (i.e., parallel to one of the crystal faces, as depicted in the sketch of Figure 3). In this situation, the field is never applied exactly along the anisotropy *z* axis of any of the molecular orientations because it is likely located in the N1−Mn−N2 molecular planes, which are tilted away from the *ac* plane by 15.85°.

To account for the possible misalignment between the molecular anisotropy axes and the crystal faces, the orientation of the main axes of the zfs tensor is left to be determined by the Euler angles α, β, and γ (=0°). The best fits of the data presented in Figure 3 were indeed achieved for α = 15.85° (and β = 55 and 145° for orientations A and B, respectively). One must keep in mind that the small deviations between the experimental and calculated results may be a consequence of the uncertainty in the alignment of the crystal with respect to the main axes of the magnet used to obtain the spectra. In addition, the presence of the two molecular orientations within the crystal complicates the analysis because the two resulting modulations superimpose for several angles.

To show this, Figure 4 includes the 336 GHz modulation of the $m_s = (-{}^3/_2 \rightarrow -{}^1/_2)$ (low-field data) and $m_s = (-{}^1/_2 \rightarrow {}^1/_2)$

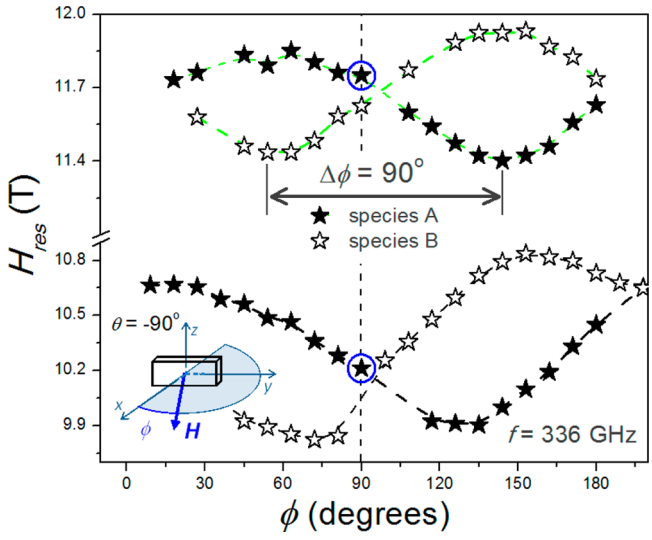

Figure 4. EPR absorption peaks obtained by rotating the magnetic field within the *xy* plane, which contains the crystal's physical longest axis. The dual modulation observed in the data corresponds to the response of the two molecular orientations in the crystal. The blue circles indicate the correspondence with the data obtained in the *zx*-plane rotation shown in Figure 3.

(high-field data) spin transitions resulting from a second rotation, orthogonal to the one shown in Figure 3, which was performed by rotating the field by an angle ϕ within the *xy* plane (θ = −90°; blue plane in the sketch of Figure 4). The data along the vertical dashed line in Figure 4 (black stars enclosed by blue circles) correspond to the data shown in Figure 3 (blue-circled stars at ϕ = 90°). The weak but dual 2-fold modulation (ΔH ~0.5 T) of the data corresponds to EPR

dx.doi.org/10.1021/ic4030958 | Inorg. Chem. 2014, 53, 5423−5428

absorptions coming from the two manganese molecular orientations within the crystal. The ∼90° shift between the two modulation patterns establishes that the anisotropy z axes of the molecules are located in the N1−Mn−N2 planes such that their projections into the xy plane are shifted by 90°. This modulation is indicative of the magnetic field being rotated slightly away from the easy-anisotropy plane of the molecules, for which the anisotropy axes of the molecules need to be rotated by the Euler angles given above (with the corresponding 90° shift in the respective β values). Note that the value of α agrees with the orientation of the N1−Mn−N2 planes with respect to the mirror ac plane and leads to a fit of the θ-rotation data in Figure 3 up to a high degree of accuracy but can only account for a 0.2 T modulation in the ϕ-rotation data of Figure 4 (not shown). It is not possible to conclude about the exact orientation of the axial symmetry axis of the molecule from the EPR measurements because we do not have face-indexed X-ray diffraction data, so that it lies within the N1−Mn−N2 plane is just a fair guess. In addition, the complexity of the EPR spectra resulting from the presence of two molecular orientations does not permit a better determination of their relative disposition with respect to the crystal from the experimental data (e.g., the dual modulation is difficult to distinguish at 239 GHz), other than the fact that the projections of their main anisotropy axes into the xy plane are shifted by ∼90°, in agreement with the spatial disposition obtained from X-ray diffraction data. Nevertheless, the data and analysis presented in this work are sufficiently clear to demonstrate the strong anisotropic nature of this mononuclear manganese compound, which is the main purpose of this work.

Pulse EPR spectroscopy was also employed to determine the characteristic spin−spin relaxation time of this system. Spin−echo measurements and the consequent echo decay were studied via HF-EPR as a function of the temperature and magnetic field orientations at 240 GHz. The experiments were performed using a two-pulse echo sequence ($p_1-\tau-p_2-\tau-$echo), where the delay τ between pulses was varied. Both pulses were 140 ns in length to optimize the echo amplitude and time resolution, for a maximum incident power on the sample of 20 mW. The initial τ = 210 ns. Echo signals were only observed at the lowest achievable temperature (1.5 K) for the $m_s = -{}^3/_2$ to $-{}^1/_2$ transition when a large part of the decoherence due to electron-spin fluctuations is quenched,[20] with an exponential decay for this sample characterized with T_2 = 500 ns (see Figure 5). Note that this is a high-concentration compound where T_2 relaxation due to dipolar electron−electron spin dominates. This relaxation pathway can be quenched at high electron-spin polarizations.[20] This effect has been observed in several single-crystalline iron-based molecular magnets, but no spin−spin relaxation has so far been measured directly in manganese-based molecular magnets. This work has relevance to that. Spin−echo spectroscopy was also performed by monitoring the echo intensity as a function of the magnetic field at different orientations within the zx plane of the crystal, similar to the continuous-wave (CW) measurements shown in Figure 3. The inset to Figure 5 shows the corresponding magnetic field values of the maximum echo intensity and its fit using the Hamiltonian of eq 1 with the same parameters as those used above.

CONCLUSIONS

We have reported the synthesis of a water-stable manganese(IV) mononuclear compound with $t_{1/2}$ ∼ 6.8 days. Most of the previously reported complexes are either water-insoluble or highly unstable in aqueous solution. Detailed single-crystal HF-EPR spectroscopy measurements show that the manganese(IV) ion presents an $S = {}^3/_2$ ground spin state with a strong axial anisotropy of the easy-anisotropy plane type. Mononuclear manganese(IV) complexes are known to exhibit moderate magnetic anisotropies (a few gigahertz). The current sample presents large single-ion anisotropy, setting the record of mononuclear manganese(IV) complexes reported so far. In addition, spin−echo experiments reveal a spin−spin relaxation time T_2 ∼ 500 ns. Although this molecule is not a SMM, its strong anisotropic character and its stability in water may enable future technological applications.

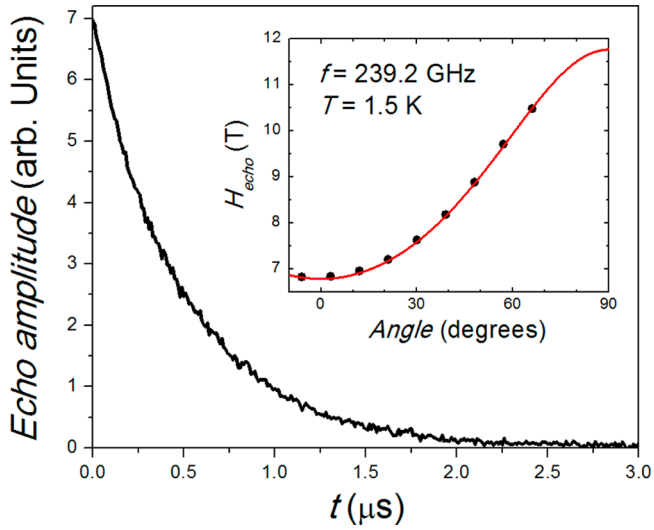

Figure 5. Exponential decay of the spin−echo amplitude measured at 239.2 GHz and 1.5 K. The inset shows the angular variation of the field position of the echo, following the same anisotropic behavior observed in the CW EPR measurements.

ASSOCIATED CONTENT

Supporting Information

Crystallographic data in CIF format (CCDC 947606), hydrogen-bonding interactions, BVS calculations, and kinetic trace for the decomposition of [Mn(L)]. This material is available free of charge via the Internet at http://pubs.acs.org.

AUTHOR INFORMATION

Corresponding Authors

*E-mail: delbarco@physics.ucf.edu.

*E-mail: mali@chemistry.jdvu.ac.in.

Author Contributions

‡These authors contributed equally to this work. M.D. with the chemical synthesis and A.A. with the physical characterization.

Notes

The authors declare no competing financial interest.

ACKNOWLEDGMENTS

M.A. acknowledges financial support from CSIR [Grant 02(2490)/11/EMR-II], UGC [Grant 39-735/2010(SR)], and DST (Grant SR/S1/IC-20/2012), New Delhi, India. M.D. thanks UGC for a SRF fellowship. A.A. and E.d.B. acknowledge support from the National Science Foundation (Grant ECCS-1001755). We are grateful to Stephen Hill for his support while these experiments were being performed at the NHMFL. Work

at the NHMFL is supported by the National Science Foundation (Grant DMR1157490), the State of Florida, and the U.S. Department of Energy.

REFERENCES

(1) (a) Kono, Y.; Fridovich, I. *J. Biol. Chem.* **1983**, *258*, 6015. (b) Algood, G. S.; Perry, J. J. *J. Bacteriol.* **1986**, *168*, 563. (c) Fronko, R. M.; Penner-Hahn, J. E.; Bender, C. J. *J. Am. Chem. Soc.* **1988**, *110*, 7554.
(2) (a) Renger, G. *Angew. Chem., Int. Ed. Engl.* **1987**, *26*, 643. (b) Pecoraro, V. L., Ed. *Manganese Redox Enzymes*; VCH Publishers: New York, 1992.
(3) (a) Yachandra, V. K.; DeRose, V. J.; Latimer, M. J.; Mukherji, I.; Sauer, K.; Klein, M. P. *Science* **1993**, *260*, 675. (b) Yachandra, V. K.; Sauer, K.; Klein, M. P. *Chem. Rev.* **1996**, *96*, 2927.
(4) (a) Sessoli, R.; Gatteschi, D.; Caneschi, A.; Novak, M. A. *Nature* **1993**, *365*, 141. (b) Wang, S.; Tsai, H.-L.; Libby, E.; Folting, K.; Streib, W. E.; Hendrickson, D. N.; Christou, G. *Inorg. Chem.* **1996**, *35*, 7578.
(5) Das, G.; Bharadwaj, P. K.; Ghosh, D.; Chaudhuri, B.; Banerjee, R. *Chem. Commun.* **2001**, 323.
(6) Lynch, M. W.; Hendrickson, D. N.; FitzgeraId, B. J.; Pierpont, C. G. *J. Am. Chem. Soc.* **1984**, *106*, 2041.
(7) (a) Pavacik, P. S.; Huffman, J. C.; Christou, G. J. *J. Chem. Soc., Chem. Commun.* **1986**, 43. (b) Mullins, C. S.; Pecoraro, V. L. *Coord. Chem. Rev.* **2008**, *252*, 416.
(8) Kessissoglou, D. P.; Butler, W. M.; Pecoraro, V. L. *J. Chem. Soc., Chem.Commun.* **1986**, 1253.
(9) Kessissoglou, D. P.; Li, X. H.; Butler, W. M.; Pecoraro, V. L. *Inorg. Chem.* **1987**, *26*, 2487.
(10) (a) Kiriya, D.; Nakamura, K.; Chang, H.-C.; Kitagawa, S. *Chem. Commun.* **2009**, 4085. (b) Lynch, M. W.; Hendrickson, D. N.; FitzgeraId, B. J.; Pierpont, C. G. *J. Am. Chem. Soc.* **1984**, *106*, 2041. (c) Attia, A. S.; Pierpont, C. G. *Inorg. Chem.* **1995**, *34*, 1172. (d) Attia, A. S.; Jung, O.-S.; Pierpont, C. G. *Inorg. Chim. Acta* **1994**, *226*, 91.
(11) (a) Chandra, S. K.; Chakravorty, A. *Inorg. Chem.* **1992**, *31*, 761. (b) Chan, M. K.; Armstrong, W. H. *Inorg. Chem.* **1989**, *28*, 3111. (c) Quee-Smith, V. C.; DelPizzo, L.; Jureller, S. H.; Kerschner, J. L. *Inorg. Chem.* **1996**, *35*, 6461. (d) Philouze, C.; Blondin, G.; Girerd, J.-J.; Guilhem, J.; Pascard, C.; Lexa, D. *J. Am. Chem. Soc.* **1994**, *116*, 8557.
(12) Duboc, C.; Collomb, M.-N. *Chem. Commun.* **2009**, 2715 and references cited therein.
(13) (a) Davies, J. J.; Smith, S. R. P.; Wertz, J. E. *Phys. Rev.* **1969**, *178*, 608. (b) Wei, Q.; Yang, Z.-Y. *Solid State Commun.* **2008**, *146*, 307 and references cited therein.
(14) Stoyanova, R.; Barra, A.-L.; Yoncheva, M.; Kuzmanovaa, E.; Zhecheva, E. *Dalton Trans.* **2011**, *40*, 9106.
(15) Weyhermüller, T.; Paine, T. K.; Bothe, E.; Bill, E.; Chaudhuri, P. *Inorg. Chim. Acta* **2002**, *337*, 344.
(16) Maity, D.; Jana, A. D.; Debnath, M.; Hearns, N. G. R.; Sie, M.-H.; Lee, H. M.; Clérac, R.; Ali, M. *Eur. J. Inorg. Chem.* **2010**, 3484.
(17) (a) *SMART*, version 5.628; *SAINT*, version 6.45a; *XPREP*; and *SHELXTL*; Bruker AXS Inc.: Madison, WI, 2004. (b) Sheldrick, G. M. *SADABS*, version 2.03; University of Gottingen: Gottingen, Germany, 2002. (c) *SHELXS-97*: Sheldrick, G. M. *Acta Crystallogr.* **2008**, *A64*, 112. (d) Spek, A. L. *Acta Crystallogr.* **2009**, *D65*, 148.
(18) Van Tol, J.; Brunel, L.-C.; Wylde, R. J. *RSI* **2005**, *76*, 074101.
(19) Morley, G. W.; Brunel, L.-C.; Van Tol, J. *RSI* **2008**, *79*, 064703.
(20) Takahashi, S.; Hanson, R.; van Tol, J.; Sherwin, M. S.; Awschalom, D. D. *Phys. Rev. Lett.* **2008**, *101*, 047601.